Journal of Solid and Fluid Mechanics (JSFM), 16(4): 1-6, 2026

Shahrood University of Technology

Journal of Solid and Fluid Mechanics (JSFM)

DOI: 10.22044/jsfm.2026.16871.4012

Manufacturing Engineering of Iran

Simulation of Turbulent Mixed Convection Heat Transfer LBE Liquid Metal Using Turbulence Models and Comparison with DNS Results

Abbas Mollaei[1], Ahmad Reza Rahmati[2,*], Hossein Khorasanizadeh [3,*]

[1] PhD Student, Department of Mechanical Engineering, University of Kashan, Kashan, Iran

[2,*] Assoc. Prof., Department of Mechanical Engineering, University of Kashan, Kashan, Iran

[3,*] Prof., Department of Mechanical Engineering, University of Kashan, Kashan, Iran

*Corresponding authors: ar_rahmati@kashanu.ac.ir, Khorasan@kashanu.ac.ir

Received: 09/22/2025 Revised: 12/27/2025 Accepted: 04/29/2026

Abstract

In this study, turbulent flow and heat transfer of a liquid metal in a vertical channel with hot and cold walls and a through-flow under buoyancy effects have been investigated. The main novelty of this study is to provide a comprehensive evaluation of the performance of various RANS turbulence models in reproducing the flow behavior at different Richardson numbers using DNS data, as well as improving the accuracy of the GEKO model through targeted adjustment of the CNW parameter. The analyses have been performed for three Richardson numbers of 0.25, 0.5, and 1. The results indicate that increasing the Richardson number intensifies the buoyancy effect on the velocity structure and temperature distribution. For Richardson numbers of 0.25 and 0.5, the SST k-ω, BSL k-ω, and k-ε Re-Enhanced models show the closest agreement with DNS data near the hot wall, with errors below 2%. The k-ε Re-Enhanced model, however, overpredicts u^+ values near the cold wall due to buoyancy effects and reduced flow velocity, resulting in lower accuracy in reproducing the near-wall flow. On the cold wall side, although all RANS models have limited capability in accurately reproducing the DNS velocity field, the SST k-ω model provides better results across the examined Richardson number range. The temperature field analysis reveals that all models successfully reproduce the overall trends of the DNS results. The results also show that adjusting the CNW parameter in the GEKO model, reducing it to -2 near the hot wall and increasing it to +2.5 near the cold wall, significantly improves prediction accuracy, and in some regions even yields performance closer to DNS than the other models. These results emphasize the importance of selecting an appropriate turbulence model and optimizing its corrective parameters when simulating turbulent flows under buoyancy effects. Data analysis indicates that the SST k-ω model exhibits superior accuracy in reproducing the velocity and temperature fields across the different Richardson number ranges examined (0.25, 0.5, and 1), while the GEKO model with optimized CNW is capable of substantially enhancing prediction accuracy in sensitive regions of the flow.

Keywords: Turbulent Flow, Mixed Convection Heat Transfer, Turbulence Models, DNS (Direct Numerical Simulation)

1. Introduction

Turbulent flow in liquid metals is characterized by irregular motion and complex fluid fluctuations, and it plays a key role in heat transfer and effective mixing. Accurate analysis of this type of flow is of great importance because these fluctuations enhance the rate of energy and heat transfer, thereby improving the performance of thermal systems. This issue is particularly significant in systems that utilize liquid metals for heat transfer, such as electronic cooling equipment and energy systems that require high heat dissipation. In the following two subsections, previous studies are reviewed in two categories: microchannel heat sinks using liquid metals, and turbulent flow and heat transfer in liquid metals.

Hodes et al. [1] showed that using Galinstan in microchannel heat sinks can reduce thermal resistance by up to about 40% compared with water..

Mollaei and Rahmati [2] found that in a single-channel active heat sink using Galinstan, an upward flow direction at Richardson number 1 and without a magnetic field increases the Nusselt number by about

11.32% compared to the downward flow direction..

Mollaei and Rahmati [3] investigated forced convective heat transfer of the liquid metal Galinstan in a ten-channel heat sink under magnetic fields with different Hartmann numbers. Their results showed that when the magnetic field is applied in the y-direction, perpendicular to the fluid flow, the Lorentz force has a stronger influence on the flow. At a Hartmann number of 88, applying the magnetic field in the y and z directions increases the convective heat transfer coefficient by about 15% and 8%, respectively.

Mollaei and Rahmati [4] investigated the flow behavior of a liquid metal under a magnetic field in a single-channel heat sink. Their results showed that applying a uniform magnetic field produces an M-shaped velocity profile. This velocity distribution increases the flow velocity near the channel walls, leading to a higher velocity gradient and consequently increased friction.

Turbulent flow, characterized by strong fluctuations and mixing, is crucial in many engineering applications, particularly thermal and fluid systems. Despite its modeling complexity, it significantly enhances heat and mass transfer, making it essential for optimizing devices such as electronic cooling systems, heat exchangers, and reactors.

Albets et al. [5] showed that applying a magnetic field to turbulent liquid-metal flow in a circular pipe significantly suppresses turbulence and generates Lorentz-force-induced instabilities in the magnetic boundary layer.

Fico et al. [6] showed that a transverse magnetic field induces turbulence anisotropy and mixed quasi-2D/3D structures in pipes, and regenerates turbulence in channels due to the conductivity of Hartmann walls.

Alemany et al. [7] experimentally and theoretically investigated magnetohydrodynamic (MHD) turbulence at low magnetic Reynolds numbers. Their results showed that an external magnetic field produces anisotropic dissipation, which is independent of the wavenumber and can be characterized by the initial interaction parameter N_0.

Zikanov et al. [8] used large-eddy simulation (LES) with the dynamic Smagorinsky model to study decaying turbulence of an electrically conducting fluid under a uniform magnetic field. The results showed that in the later stages of decay, viscous and Joule dissipation contribute nearly equally to the kinetic energy loss, while the parallel and perpendicular velocity components decay at different rates, indicating strong small-scale anisotropy in the turbulent flow.

Levchenya et al. [9] showed that 45° ribs enhance heat transfer in a rectangular channel, although they also increase pressure drop**.**

Araseki et al. [10] developed a numerical approach for simulating turbulent MHD liquid-metal flow in a rectangular channel under a transverse magnetic field. The method iteratively enforced the conservation of electric current density and employed the Bulatov turbulence model to compute turbulence intensity and shear stresses. The results showed good agreement with experimental data, confirming the method's effectiveness.

Due to the high computational cost of direct numerical simulation (DNS), comparing DNS data with turbulence models provides an effective approach for improving the simulation of turbulent flows in liquid metals. This study numerically investigates fully turbulent flow and mixed convection heat transfer in a vertical channel containing a liquid metal. The research focuses on evaluating the performance of different turbulence models (SST k-ω, BSL k-ω, k-ε Re-Enhanced, and GEKO) under various Richardson numbers and comparing their predictions with DNS data.

2. Methodology

Figure 1 shows a vertical planar channel similar to that studied by Pucciarelli et al. [11], where the z-direction is neglected and the problem is considered two-dimensional. The geometric parameters used in this study are a channel height of L= 10 m and a channel half-width of δ = 0.0178 m

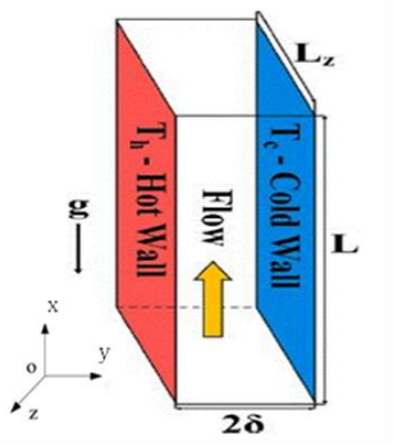


Figure 1. Coordinate system and flow geometry.

This study employed two-dimensional RANS simulations to reduce the computational cost compared with DNS. A 10 m long channel was considered to ensure fully developed flow. The mesh was uniform along the streamwise direction and refined near the walls to satisfy the condition y+ < 1. Grid independence was also examined. The governing equations were solved in ANSYS Fluent using the SIMPLEC algorithm with second-order spatial discretization.

3. Discussion and Results

In this study, the dimensionless transverse coordinate y is used to present the results, where the negative side represents the buoyancy-assisting region and the positive side represents the buoyancy-opposing region.

Velocity and temperature are also defined in dimensionless form. The results at Ri = 0.25 show that buoyancy increases the velocity on the assisting side and decreases it on the opposing side. Comparison with DNS data indicates that k-omega-based models, particularly SST and BSL, predict the flow behavior and near-wall region more accurately than other RANS models.

Figures 2 and 3 present the dimensionless velocity distributions for the operating condition with the Richardson number Ri = 0.25. The results show that even at this relatively low value of Ri, the influence of buoyancy forces on the velocity field is significant. Specifically, on the buoyancy-assisting side of the flow, fluid acceleration near the wall leads to higher local velocities, whereas on the buoyancy-opposing side, buoyancy has a suppressing effect and reduces the flow velocity. This reduction in velocity on the opposing side results in a lower wall shear stress and, consequently, larger values of the dimensionless velocity u_plus compared with the hot-wall side.

Comparison with DNS data indicates that, near the hot wall, the SST k-omega, BSL k-omega, and k-epsilon Re-Enhanced models reproduce the flow behavior with reasonable accuracy due to their ability to capture strong gradients of velocity and wall shear stress. In contrast, near the cold wall, the simultaneous presence of velocity reduction and buoyancy effects complicates the boundary-layer structure and limits the accuracy of most RANS models. Among these models, only the k-omega-based approaches, including SST and BSL, provide acceptable agreement with the DNS results because of their higher sensitivity to the near-wall region. These findings highlight the superiority of k-omega models for simulating mixed convection flows, especially in regions where buoyancy effects are strong.

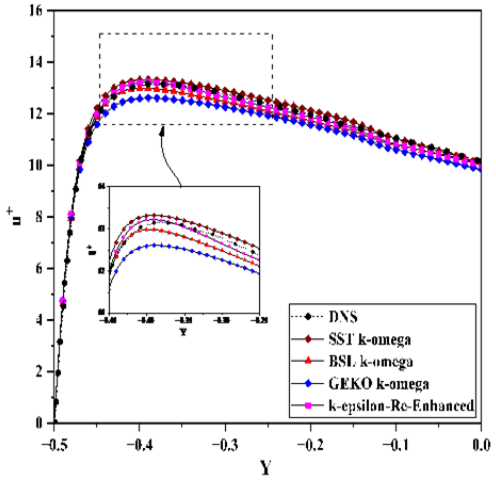


Figure 2. Dimensionless velocity obtained from DNS and RANS results on the buoyancy-assisting side for Ri = 0.25

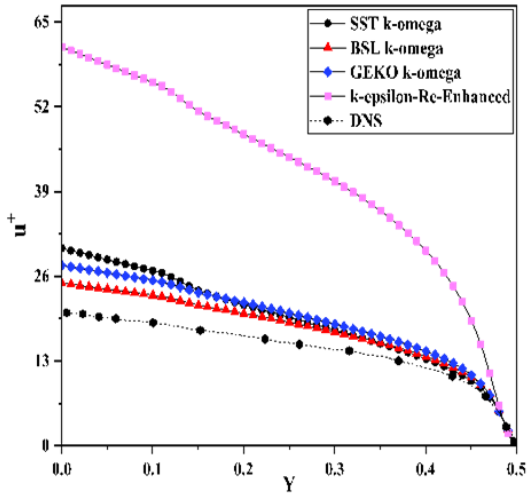


Figure 3. Dimensionless velocity obtained from DNS and RANS results on the buoyancy-opposing side for Ri = 0.25

The results shown in Figure 4 indicate that all of the evaluated turbulence models are able to accurately predict the dimensionless temperature distribution on both the hot and cold walls, successfully reproducing the overall trend of the DNS data. This favorable performance can be attributed to the dominance of conduction-controlled heat transfer in the near-wall regions and to the lower sensitivity of the temperature field to the detailed turbulent fluctuations. In contrast to the velocity field, which is strongly influenced by turbulent structures and shear stresses, the temperature distribution in this regime is primarily governed by the wall temperature gradient and the imposed boundary conditions. As a result, even lower-complexity RANS models are capable of providing an acceptable representation of the temperature field on both walls.

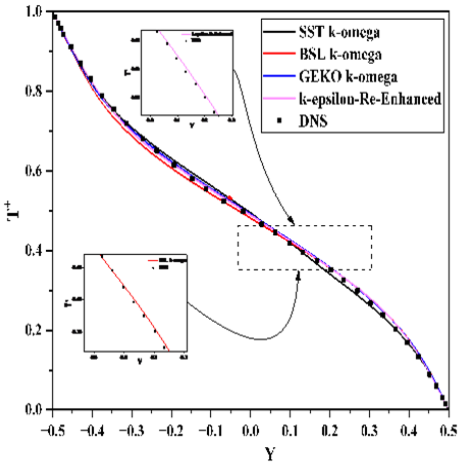


Figure 4. Dimensionless temperature obtained from DNS and RANS results across the entire flow domain for Ri = 0.25

The velocity and temperature contours presented in Figures 5 and 6 for the Richardson number Ri = 0.25 show that all turbulence models predict a clear difference

between the regions adjacent to the hot and cold walls. In the velocity field, the dominance of buoyancy effects near the hot wall strengthens the shear stress and increases the local velocity, whereas a reduction in flow intensity is observed near the cold wall. This behavior highlights the determining role of buoyancy in shaping the asymmetric structure of the flow field even at relatively low values of Ri.

A comparison of the patterns predicted by the models shows that the SST k-omega model provides a balanced velocity distribution and exhibits a milder response to buoyancy effects. In contrast, the BSL k-omega model intensifies the velocity gradient near the hot wall and predicts a more pronounced difference between the two walls. The GEKO model reproduces a more uniform velocity field and reduces the gradient intensity between the walls, while the k-epsilon Re-Enhanced model predicts the largest velocity difference between the hot and cold walls, indicating the highest sensitivity to buoyancy forces.

Overall, the analysis of the velocity contours indicates that the different turbulence models exhibit varying levels of response to buoyancy effects, such that the SST k-omega model predicts the mildest velocity gradients, whereas the k-epsilon Re-Enhanced model predicts the strongest velocity gradients in the flow field.

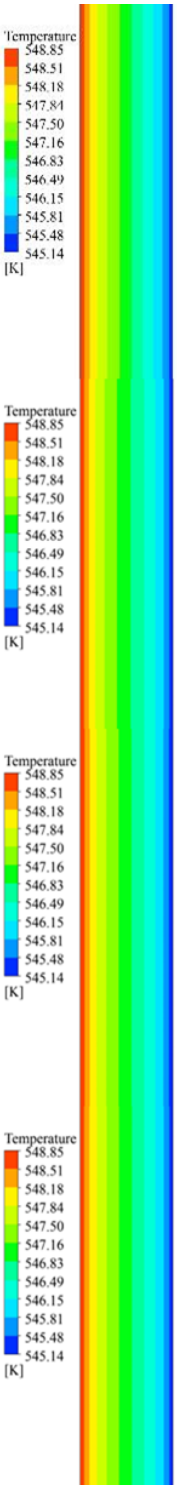


Figure 5. Velocity contours for the four turbulence models, namely SST k-omega, BSL k-omega, GEKO k-omega, and k-epsilon Re-Enhanced, at Ri = 0.25

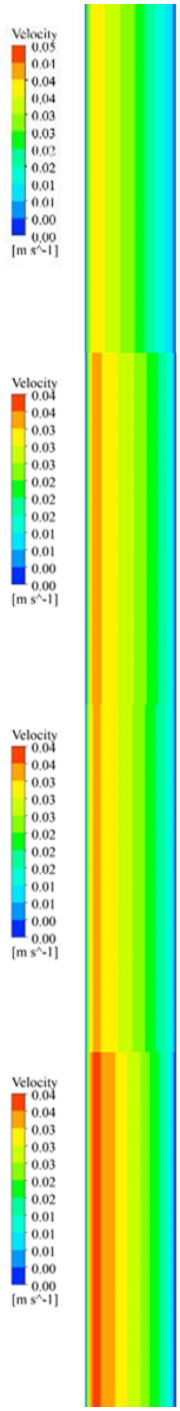


Figure 6. Temperature contours for the four turbulence models, namely SST k-omega, BSL k-omega, GEKO k-omega, and k-epsilon Re-Enhanced, at Ri = 0.25

One of the turbulence models examined in this study is the GEKO model, which shows acceptable performance near the hot wall and provides reasonable results. However, compared with the other three models, namely SST k-omega, BSL k-omega, and k-epsilon Re-Enhanced, it exhibits a larger deviation from the DNS data.

Figure 7 presents the results of the GEKO model for different values of the CNW parameter at Ri = 0.25 in the region near the hot wall. Reducing the CNW value to −2 and −2.5 improved the model's ability to predict the flow behavior in this region and, at certain locations, produced results that were more accurate than those obtained with the other three turbulence models. In general, the CNW parameter controls the sensitivity of the model to the flow behavior in near-wall regions, and selecting an appropriate value can significantly improve the prediction accuracy in the vicinity of the hot wall.

In contrast, near the cold wall, the flow is calmer and the intensity of buoyancy effects is lower. In this region, increasing the CNW value up to 2.5 improves the performance of the model in reproducing the flow behavior, and the predictions show better agreement with the DNS results, as illustrated in Figure 8. In other words, the CNW parameter controls the sensitivity of the model to near-wall phenomena, and its optimal value is not the same for the hot and cold walls. This highlights the importance of carefully tuning CNW to enhance the accuracy of the GEKO model in different regions of the flow.

Figure 9 shows the dimensionless temperature distribution predicted by the GEKO turbulence model. By reducing the CNW value to −2, the model predictions exhibit improved agreement with the DNS data, and the temperature variation across the channel width is reproduced with good accuracy in most regions. These results indicate that appropriate adjustment of the CNW parameter enhances the representation of near-wall thermal gradients and improves the capability of the GEKO model to predict the detailed temperature field under the influence of strong buoyancy effects.

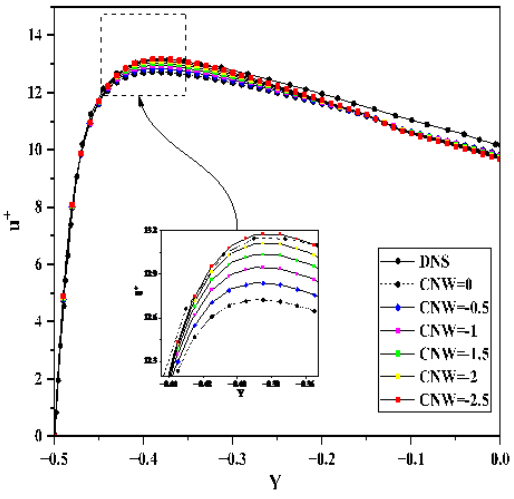


Figure 7. Dimensionless velocity obtained from DNS and GEKO results on the buoyancy-assisting side for Ri = 0.25 with different CNW values

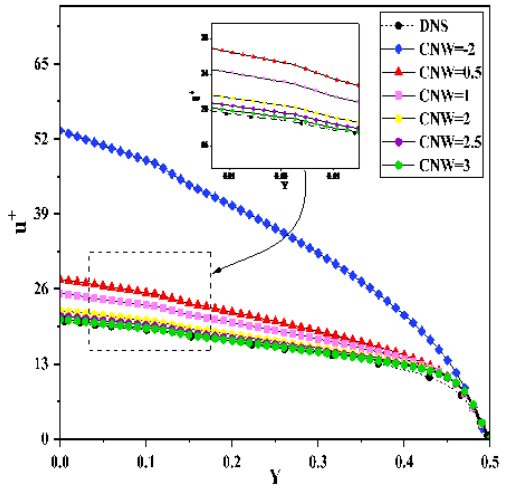


Figure 8. Dimensionless velocity obtained from DNS and GEKO results on the buoyancy-opposing side for Ri = 0.25 with different CNW values

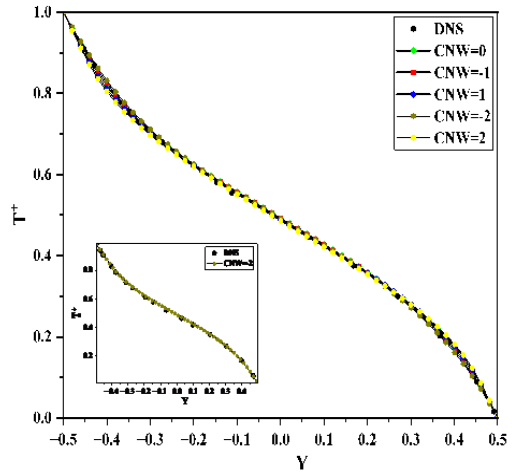


Figure 9. Dimensionless temperature obtained from DNS and RANS results across the entire flow domain for Ri = 0.25 with different CNW values

5. References

[1] Hodes, M., Zhang, R., Lam, L. S., Wilcoxon, R., & Lower, N. (2013). On the potential of galinstan-based minichannel and minigap cooling. *IEEE Trans. Compon. Packag. Manuf. Technol*., 4(1), 46-56.

[2] Molaei, A., & Rahmati, A. R. (2024). Improvement of mixed convection heat transfer of liquid metal in a single channel heat sink under uniform external magnetic field. *J. Solid Fluid Mech*., 14(2), 77-94.

[3] Rahmati, A. R., & Molaei, A. (2024). Investigation on the effect of magnetic field on forced convection heat transfer of liquid metals in a microchannel heat sink. *J. Comput. Methods Eng*., 42(2), 149-166.

[4] Rahmati, A. R., & Mollaei, A. (2024). Numerical simulation of forced convection heat transfer of liquid metals in a microchannel heat sink under a magnetic field. *J. Struct. Fluid Mech*., 13(6), 121-137.

[5] Albets-Chico, X., Grigoriadis, D. G. E., Votyakov, E. V., & Kassinos, S. (2013). Direct numerical simulation of turbulent liquid metal flow entering a magnetic field. *Fusion Eng. Des*., 88(12), 3108-3124.

[6] Fico, F., Xia, H., & Langella, I. (2025). Magnetohydrodynamic Turbulence in Bounded Liquid Metal Flows. In Cambridge Unsteady Flow Symposium (pp. 439-453). *Springer, Cham*.

[7] Alemany, A., Moreau, R., Sulem, P. L., & Frisch, U. (1979). Influence of an external magnetic field on homogeneous MHD turbulence. *J. Mec*., 18(2), 277-313.

[8] Burattini, P., Zikanov, O., & Knaepen, B. (2010). Decay of magnetohydrodynamic turbulence at low magnetic Reynolds number. *J. Fluid Mech*., 657, 502-538

[9] Levchenya, A. M., Galaev, S. A., & Ris, V. V. (2025). Influence of the Prandtl Number on Heat Transfer Intensification in a Developed Turbulent Flow in a Channel with One Finned Wall. *J. Eng. Phys. Thermophys*., 1-10.

[10] Araseki, H., & Kotake, S. (1994). Numerical method for analysis of turbulent liquid metal magnetohydrodynamic flow. *Nucl. Eng. Des*., 152(1-3), 231-241.

[11] Pucciarelli, A., Shams, A., & Forgione, N. (2023). Numerical prediction of turbulent flow and heat transfer in buoyancy-affected liquid metal flows. *Ann. Nucl. Energy*, 186, 109773.